Forward Uncertainty Quantification and Sensitivity Analysis of the Holzapfel-Ogden Model for the Left Ventricular Passive Mechanics

Berilo de Oliveira Santos[1[0000−0002−3870−5474]], Rafael Moreira Guedes[1[0000−0003−3625−8284]], Luis Paulo da Silva Barra[1[2222−−3333−4444−5555]], Raphael Fortes Marcomini[1[0000−0003−2608−8082]], Rodrigo Weber dos Santos[1[0000−0002−0633−1391]], and Bernardo Martins Rocha[1[0000−0002−0508−8959]⋆]

Universidade Federal de Juiz de Fora, Juiz de Fora, Brasil
{berilo.santos,rafael.guedes,raphael.marcomini}@engenharia.ufjf.br
{bernardomartinsrocha, rodrigo.weber}@ice.ufjf.br luis.barra@ufjf.edu.br

Abstract. Cardiovascular diseases are still responsible for many deaths worldwide, and computational models are essential tools for a better understanding of the behavior of cardiac tissue under normal and pathological situations. The microstructure of cardiac tissue is complex and formed by the preferential alignment of myocytes along their main axis with end-to-end coupling. Mathematical models of cardiac mechanics require the process of parameter estimation to produce a response consistent with experimental data and the physiological phenomenon in question. This work presents a polynomial chaos-based emulator for forward uncertainty quantification and sensitivity analysis of the Holzapfel-Ogden orthotropic constitutive model during the passive filling stage. The fiber orientation field is treated as a random field through the usage of the Karhunen-Loève (KL) expansion. The response and uncertainty of the constitutive parameters of the model considered here are also investigated. Our results show the propagated uncertainties for the end-diastolic volume and fiber strain. A global sensitivity analysis of the constitutive parameters of the complete model is also presented, evidencing the model's key parameters.

Keywords: Cardiac Mechanics · Karhunen-Loève Expansion · Polynomial Chaos

1 Introduction

Cardiovascular diseases are the leading cause of death in the world, however, many of them can be avoided if there is a previous diagnosis. Computational

⋆ Supported by UFJF, CAPES, CNPq (Grants 310722/2021-7, 315267/2020-8), and FAPEMIG (Grants APQ-01340-18, APQ 02489/21).

ICCS Camera Ready Version 2022
To cite this paper please use the final published version:
DOI: 10.1007/978-3-031-08760-8_61

models are essential tools to understand better the cardiac system and, above all, how it is affected by pathologies or disorders [13]. Cardiac tissue is made up of fibers that are fundamental in various aspects of the heart, and therefore, changes in its typical orientation can result in improper functioning, as is the case with hypertrophic cardiomyopathy (HCM) [12] that affects the heart muscle. HCM is responsible for the thickening of the cardiac muscle (especially the ventricles or lower heart chambers), increased left ventricular stiffness, fiber disarray, and cellular changes [9].

During the last years, computational models of the cardiovascular system have evolved significantly. In particular, the construction of patient-specific models that could be applied in the clinical setting is a high goal. However, the construction of patient-specific models involves several sources of uncertainty, ranging from personalized geometries based on medical images to parametric uncertainty inherent in the underlying mathematical model.

Recently, many studies on uncertainty quantification for cardiac electromechanics have been performed [14, 15, 4, 3, 10]. The work of [14] was one of the first to apply uncertainty quantification (UQ) techniques for the problem of passive filling of the left ventricle (LV). They considered as inputs the constitutive parameters of a transversely isotropic constitutive model [6]. In [15] similar analyses were carried out, but now considering the fiber orientation field as a random field through the KL expansion. In [4] another source of uncertainty was added in the LV model, where geometry was also considered as uncertain through a parametrized strategy for mesh generation. The previous studies focused on the passive filling phase of the LV only. A sensitivity analysis and forward uncertainty quantification study of the complete cardiac cycle was presented in [3]. In [10] a sensitivity analysis of a detailed human fully-coupled ventricular electromechanical model was conducted using the HO model. However, due to the usage of a more complex coupled electromechanical model with many parameters, only one parameter of the HO model was evaluated.

In this work, we focus on forward uncertainty quantification and sensitivity analysis of the passive filling phase of the left ventricular mechanics. We considered as uncertain input parameters the parameters from the Holzapfel-Ogden (HO) constitutive model [7] and the fiber field as a random field using the truncated Karhunen-Loève (KL) expansion. The analyses were performed using surrogate models (emulators) based on the Polynomial Chaos Expansion (PCE), as in previous works on cardiac mechanics [3, 4].

The remaining of this manuscript is organized as follows: in section 2 the mathematical models, the numerical methods, the techniques used for uncertainty quantification, and sensitivity analysis are presented. Next, section 3 describes the computer implementation and computational experiments; while the numerical results are presented on section 4. Section 5 ends this work with conclusions, limitations, and possible future works.

ICCS Camera Ready Version 2022
To cite this paper please use the final published version:
DOI: 10.1007/978-3-031-08760-8_61

2 Models and Methods

2.1 Cardiac Mechanics

The focus of this study is to model the phenomenon of cardiac mechanics that corresponds to the (passive) filling of the left ventricle (LV) by the blood during the diastolic phase. At this stage, blood fills the LV cavity and exerts pressure on the endocardial surface. The following problem describes the passive filling of the LV:

$$\nabla \cdot (\mathbf{FS}) = \mathbf{0}, \quad \text{in} \quad \Omega_0, \tag{1}$$

$$\mathbf{u} = \mathbf{0}, \quad \text{on} \quad \partial\Omega_{\text{base}}, \tag{2}$$

$$(\mathbf{FS})\mathbf{N} = p_{\text{endo}}\mathbf{F}^{-T}\mathbf{N}, \quad \text{on} \quad \partial\Omega_{\text{endo}}, \tag{3}$$

where $\mathbf{F}$ is the deformation gradient tensor, $\mathbf{S}$ is the second Piola-Kirchhoff stress tensor, $\mathbf{u}$ is the displacement field, $\mathbf{N}$ is the unit normal vector of the endocardium surface, and p_{endo} is the applied pressure on the endocardium. For simplicity, we considered zero displacement boundary conditions at the base of the endocardium.

The Holzapfel-Ogden (HO) constitutive model was used to describe the LV tissue stress-strain relationship. The strain energy function of the HO model for the incompressible case is described by:

$$\Psi = \frac{a}{2b}\left[\exp\left\{b\left(I_1 - 3\right)\right\} - 1\right] + \frac{a_f}{2b_f}\left[\exp\left\{b_f\left(\max\left(I_{4f}, 1\right) - 1\right)^2\right\} - 1\right] \tag{4}$$

where a, b, a_f, b_f, a_s, b_s, a_{fs}, and b_{fs} are the material parameters, and I_1, I_{4f}, and I_{8fs} are invariants given by: $I_1 = \text{tr}(\mathbf{C})$, $I_{4\text{f}} = \mathbf{f}_0 \cdot (\mathbf{C}\mathbf{f}_0)$, $I_{4\text{s}} = \mathbf{s}_0 \cdot (\mathbf{C}\mathbf{s}_0)$, $I_{8\text{fs}} = \mathbf{m}_0 \cdot (\mathbf{C}\mathbf{s}_0)$ where $\mathbf{C} = \mathbf{F}^T\mathbf{F}$ is the right Cauchy-Green tensor, $\mathbf{f}_0$ and $\mathbf{s}_0$ are the fiber and sheet directions in the reference configuration, respectively. The second Piola-Kirchhoff stress tensor $\mathbf{S}$ of Eq.(1) is given by $\mathbf{S} = 2\frac{\partial\Psi(\mathbf{C})}{\partial\mathbf{C}} - p\mathbf{C}^{-1}$, where p is the pressure.

2.2 Left Ventricular Geometry and Fiber Orientation

A simplified geometric model of the left ventricle, generated from the equations of a family of a truncated ellipsoid, where the wall thickness is homogeneous, was considered. Figure 1 (left) shows its dimensions with measurements that typically represent the human LV. The finite element mesh generated from this geometry, as shown in Figure 1 (middle), is composed of a total of 1786 nodes and 6395 tetrahedral elements.

A typical fiber orientation field for the LV is illustrated on Figure 1 (right). The microstructure of the cardiac tissue is represented as a constant function per element, where each element has unit vectors $\mathbf{f}_0$, $\mathbf{s}_0$, and $\mathbf{n}_0$ that describes the fiber, sheet, and normal directions in the reference configuration. To generate the fiber orientation, the Laplace-Dirichlet Rule-Based (LDRB) rule-based algorithm

ICCS Camera Ready Version 2022
To cite this paper please use the final published version:
DOI: 10.1007/978-3-031-08760-8_61

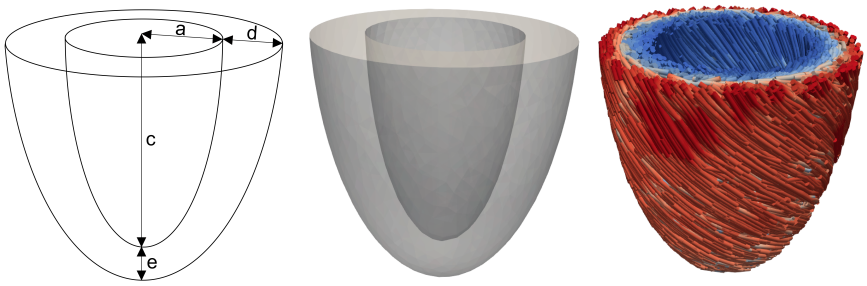

Fig. 1. The left ventricular geometry and its corresponding finite element mesh are shown on the left and middle panels; whereas a typical visualization of the fiber field orientation is shown on the right. The following dimensions were used: $a = 2.0$ cm, $c = 6.0$ cm, $d = 1.3$ cm, and $e = 1.0$ cm, which results in the approximately 50 mL of cavity volume.

developed by [1] was used. The baseline fiber orientation used in this study has a helical angle of 60° on the endocardium surface and varies linearly throughout the myocardium (transmural direction) up to the value of -60° on the epicardium surface.

2.3 Numerical Solution

Numerical solutions of the problem given in Eq. (1) were obtained by the finite element method (FEM) implemented in the open-source library FEniCS. For discretization, a mixed method of the Taylor-Hood type was used to approximate $(\mathbf{u}, p)$ with approximations $\mathbb{P}_2 \times \mathbb{P}_1$, that is, of degree 2 for the displacement field and degree 1 for the pressure field, respectively. The non-linear LV filling problem is solved with Newton's method. In addition, an incremental procedure was used and the total pressure to be applied, of $p_{endo} = 2.7$kPa, was divided into 50 steps as performed in [8].

2.4 Polynomial Chaos Expansion Surrogate Models

An emulator or surrogate model is an approach that aims to solve a complex problem in a simplified and, consequently, faster way. In the specific case of this work, an emulator based on polynomial chaos expansion (PCE) was adopted, which has been successfully used in other works [14, 4, 3] on cardiac mechanics to perform forward uncertainty quantification and sensitivity analyses.

PCE is a technique for generating low-cost computational approximations for a quantity of interest Y, usually obtained after solving the governing equations (the forward problem). Let $f(\mathbf{Z})$ be the simulator of this quantity of interest Y, where $\mathbf{Z}$ are the input parameters. This quantity is expanded into a series of

ICCS Camera Ready Version 2022
To cite this paper please use the final published version:
DOI: 10.1007/978-3-031-08760-8_61

orthogonal polynomials Ψ_j with random entries. The PCE for Y is given by:

$$Y = \sum_{j=0}^{\infty} b_j \Psi_j \left(\{Z_n\}_{n=1}^{\infty} \right) = f_{PCE}(\mathbf{Z}) \tag{5}$$

where b_j are the coefficients to be determined and Ψ_j are the orthogonal polynomials with their respective random variables $Z_1, Z_2, \ldots, Z_n$. In practice, the expansion is truncated at a finite number of terms, and the approximation of Y, obtained by the emulator f_{PCE} and denoted by $\hat{Y}$, can be expressed by:

$$f(\mathbf{Z}) = Y \approx \hat{Y} = \sum_{j=0}^{N_p - 1} c_j \Psi_j(\mathbf{Z}) = f_{PCE}(\mathbf{Z}) \tag{6}$$

where c_j are the coefficients of the expansion to be determined and $\Psi_j(\mathbf{Z})$ are the orthogonal polynomials. The polynomial expansion of Eq. (6) has degree p for D input parameters. The number of terms is given by: $N_p = \frac{(D+p)!}{D!p!}$.

For an improved accuracy of the surrogate model, it is recommended to use a number of terms (samples) greater than N_p to create it. In general, a multiplicative factor m is adopted. That is, the number of samples is given by $N_s = mN_p$. There are different ways to determine the coefficients c_j that determine the emulator of a quantity. In this work, the stochastic collocation method [14] was adopted, which together with the choice of N_s for $m > 1$ results in a least-squares problem. More details on this procedure can be found in [14, 4].

At this point, it is important to note that the emulators for the mechanical problem, defined in Eq. 1, are polynomials that approximate the outputs of the simulator. Furthermore, once the emulators are built, due to their polynomial nature, these values can be calculated cheaply by evaluating the polynomial (emulator) for a given set of parameters which makes them appropriate for forward uncertainty quantification and sensitivity analysis.

2.5 Sensitivity Analysis via Sobol

Sensitivity analysis measures the impact of input parameters on some output data of a problem. In this work, the first order and total Sobol [16] indices were adopted.

Let Y be a scalar quantity of interest for which we want to assess the impact of the input parameters $\mathbf{X} = \{X_1, X_2, \ldots, X_D\}$. The first order Sobol index expresses the direct influence of a parameter X_i on the variance of the quantity of interest Y. This index is given by:

$$Si = \frac{\mathbb{V}[\mathbb{E}(Y|X_i)]}{\mathbb{V}(Y)} \tag{7}$$

where $\mathbb{E}$ denotes the expected value, $\mathbb{V}$ represents the variance, and $\mathbb{E}(Y|X_i)$ denotes the expected value of the output Y when the parameter X_i is fixed.

ICCS Camera Ready Version 2022
To cite this paper please use the final published version:
DOI: 10.1007/978-3-031-08760-8_61

The first order Sobol sensitivity index represents the expected reduction in the variance of the analyzed quantity when the parameter X_i is fixed.

The total Sobol index represents possible interactions between the input parameters and their effects on the Y quantity. For the input X_i it is denoted by S_{Ti}, and is given by:

$$S_{Ti} = \frac{\mathbb{E}[\mathbb{V}(Y|X_{\sim i})]}{\mathbb{V}(Y)} = 1 - \frac{\mathbb{V}[\mathbb{E}(Y|X_{\sim i})]}{\mathbb{V}(Y)} \tag{8}$$

where $X_{\sim i}$ represents all input parameters except the X_i parameter.

In this work the Sobol sensitivity indices were calculated from the PCE surrogate models using the implementation of the `ChaosPy` [5] library.

2.6 Random Fiber Field

Uncertainty in the fiber field of the cardiac microstructure was considered so far, with two approaches employed in previous works [3, 15]. One way [14, 4, 3, 10] is to consider the parameters α_{endo} and α_{epi} used in the rule-based fiber generation algorithm as uncertain input parameters. The other approach treats the fiber orientation as a random field and is generated via the Karhunen-Loève expansion [15]. This approach has the advantage of considering local variations in the cardiac microstructure, in contrast to the parametric approach where such variation is not present and is only represented through the α_{endo} and α_{epi} parameters.

We consider that the orientation of the fibers (only) will be represented as a random field. Fiber orientation is considered as the sum of a random field representing a perturbation $\mathbf{F}$ and the original fiber orientation field $\mathbf{f}_{micro}$ that follows the properties of the microstructure of cardiac tissue. Then, the orientation of the fibers is given by

$$\mathbf{f}(\mathbf{x}, \theta) = \mathbf{f}_{micro}(\mathbf{x}) + \mathbf{F}(\mathbf{x}, \theta), \tag{9}$$

where θ represents the dependence of the perturbed field $\mathbf{f}$ on some random property. The perturbation $\mathbf{F}$ is represented as a random field using the truncated KL expansion as follows:

$$\mathbf{F}(\mathbf{x}, \theta) = \bar{\mathbf{F}}(\mathbf{x}) + \sum_{k=1}^{n_{kl}} \eta_k(\theta)\sqrt{\lambda_k}\boldsymbol{\phi}_k(\mathbf{x}), \tag{10}$$

where $\bar{\mathbf{F}}(\mathbf{x})$ is the expected value of the stochastic field in $\mathbf{x}$ and $\{\eta_k(\theta)\}$ represents a set of independent Gaussian random variables and $(\lambda_k, \phi_k(\mathbf{x}))$ are the eigenvalues and eigenfunctions of the following integral:

$$\int_D C(\boldsymbol{y}, \boldsymbol{x})\phi_i(\boldsymbol{y})\mathrm{d}\boldsymbol{y} = \lambda_i\boldsymbol{\phi}_i(\boldsymbol{x}), \tag{11}$$

where D is the domain of the cardiac tissue of interest and $C(\mathbf{y}, \mathbf{x})$ the covariance function. Without loss of generality, it is assumed that $\bar{\mathbf{F}}(\mathbf{x}) = 0$ and that the

ICCS Camera Ready Version 2022
To cite this paper please use the final published version:
DOI: 10.1007/978-3-031-08760-8_61

covariance function has the following exponential form given by:

$$C(\boldsymbol{x}, \boldsymbol{y}) = \sigma_{\mathrm{KL}}^2 \exp\left(-\frac{|\boldsymbol{x}-\boldsymbol{y}|^2}{2l_{KL}^2}\right) \quad \forall \boldsymbol{x}, \boldsymbol{y} \in D, \tag{12}$$

where σ_{KL}^2 is the variance of the field and l_{KL} is the correlation size that defines the spatial scale over which the field exhibits significant correlation [15].

In practical terms, to compute the KL expansion given in Eq. (9), the following generalized eigenvalue problem needs to be solved:

$$\mathbf{T}\boldsymbol{\phi}_k = \lambda_k \mathbf{M}\boldsymbol{\phi}_k, \quad \text{with} \quad \mathbf{T} = \mathbf{M}^T\mathbf{C}\mathbf{M}, \tag{13}$$

where $\mathbf{M}$ is the mass matrix calculated using the finite element method.

The truncated KL expansion reduces the dimensionality of the stochastic space from infinity to n_{KL} and provides a parametric representation of the random field $\mathbf{F}(\mathbf{x}, \theta)$ through n_{KL} random variables. The uncertainty (or randomness) in the fiber orientation field comes from n_{KL} independent random variables $\eta_1, \ldots, \eta_{n_{KL}}$, which follow normal distributions with mean zero and unit standard deviation, ie $\eta_i \sim \mathcal{N}(0, 1)$.

2.7 Quantities of Interest

To evaluate the parametric uncertainty in the response of the model given by Eq. 1 we considered the following outputs or quantities of interest (QoI): cavity volume (as a function of applied pressure), the end-diastolic volume (EDV), and an average fiber strain measured at the end of diastole [3]. Fiber strain was computed as:

$$\varepsilon_{fiber} = \mathbf{f}_0^T \mathbf{E} \mathbf{f}_0, \tag{14}$$

where $\mathbf{E}$ is the Green-Lagrange strain tensor and $\mathbf{f}_0$ is the fiber orientation in the undeformed configuration. The average fiber strain is computed using a set of 20 points uniformly distributed in the LV domain and Eq. (14) to compute their values.

3 Implementation and Experiments

3.1 Implementation

The computational experiments of this work were all carried out in a code implemented in the Python programming language with support for scientific computing through the `NumPy` and `SciPy` libraries. The library `ChaosPy` [5] was used for uncertainty quantification, sensitivity analysis, and the construction of the KL expansion. The library `FEniCS` [11] was used for solving the forward problem (passive filling of the LV) using finite elements. The library `ldrb` [1] was used to generate the fiber field in finite element meshes LDRB.

ICCS Camera Ready Version 2022
To cite this paper please use the final published version:
DOI: 10.1007/978-3-031-08760-8_61

3.2 Numerical Experiments

Two experiments were carried out for UQ and SA. The first one considered only the 4 input parameters of the HO model (transversely isotropic case) and no uncertainties in the fiber field. We assumed uniform distributions for the uncertain parameters of the HO model, allowing them to vary from half its reference value to a two-fold increase in the reference value. Uniform distributions were chosen due to the lack of data for parameters [4, 14, 15], and also to represent the population average values [2]. Table 1 summarizes the baseline parameters values and the corresponding distributions used in the experiments for UQ and SA.

Table 1. Baseline parameter values of the HO model and the distributions used to construct the PCE surrogate models. The uniform distributions are bounded by below and above with half and twice of the baseline value, respectively.

Parameter	a	b	a_f	b_f
Baseline value	228	7.78	116.85	11.83
Distribution	$\mathcal{U}(114, 456)$	$\mathcal{U}(3.89, 15.56)$	$\mathcal{U}(58.42, 233.7)$	$\mathcal{U}(5.92, 23.66)$

The second experiment extends the previous one, where uncertainty in the fiber field is now included in the analysis via the KL technique. The settings for the HO parameters were the same of the first experiment. For the KL expansion a total of $n_{KL} = 8$ terms was used, and the following parameters were considered: $\sigma_{KL} = 0.5$ radians and $l_{KL} = 1.0$ cm, as previously used in [15]. We considered $p = 2$ and $m = 2$, which for the first experiment with $D = 4$ resulted in $N_s = 30$ samples, whereas for the second experiment with $D = 12$ resulted in a total of $N_s = 182$ samples (train data) that were generated for the construction of the surrogate models. Finally, the accuracy of the surrogate models were carried out via a new set of $N_s^{test} = 100$ simulations (test data).

4 Results

In the following, we present the numerical results obtained in this work. First, a preliminary study to define the number of terms in the KL expansion was carried out, followed by a study to show the prediction capabilities of the PCE surrogate models employed for further analyses. Then, results of the forward UQ and SA of the passive filling LV problem using the HO model are presented.

4.1 Karhunen-Loeve Expansion

First, to define the number of terms in the truncated KL expansion for representing the random fiber field, we computed the eigenvalues of the generalized problem defined in equation (13). Figure 2 shows the first 128 eigenvalues, where it is clear their fast decay. To avoid a large number of input parameters, we adopted $n_{KL} = 8$ for further studies with random fiber fields.

ICCS Camera Ready Version 2022
To cite this paper please use the final published version:
DOI: 10.1007/978-3-031-08760-8_61

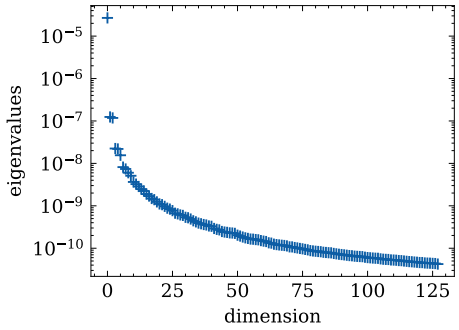

Fig. 2. Eigenvalues of the KL expansion for the LV mesh considered in this work.

4.2 Polynomial Expansion Emulator

After creating the emulator using N_s samples, a new set of N_s^{test} new samples was generated with the FEM simulator. This study aims to assess the prediction capabilities of the surrogate models on test data.

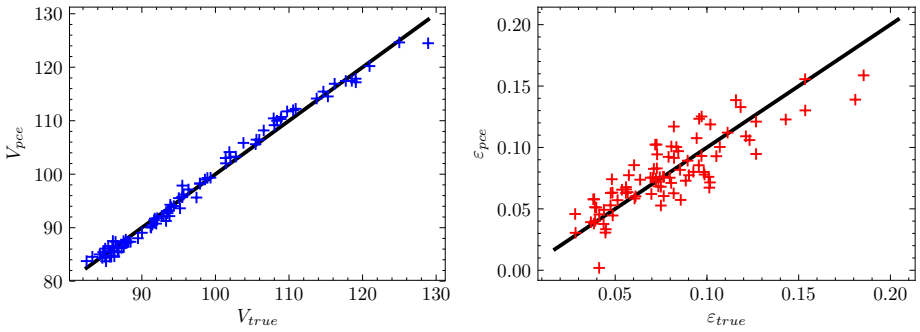

Fig. 3. Prediction results of the end-diastolic volume (left) and fiber strain (right) using the PCE surrogate model on the set of test samples.

Figure 3 shows the true values of the outputs (EDV and average fiber strain) versus the predicted values obtained by the PCE surrogate models. The black line suggests the exact predictions of the true values, while the points are the predictions. The closer the points to the solid black line, the better predictability is for the surrogate models. One can observe that the PCE surrogate models can predict the outputs very well in general.

4.3 Forward Uncertainty Quantification

Forward uncertainty quantification for experiments 1 (HO parameters only) and 2 (HO parameters and random fiber field via KL) were carried out to evaluate the

ICCS Camera Ready Version 2022
To cite this paper please use the final published version:
DOI: 10.1007/978-3-031-08760-8_61

uncertainties on the QoIs. Figure 4 (left panel) shows the propagated uncertainty to the cavity volume as a function of pressure for experiments 1 and 2, labeled as HO and HO+KL, which consider as input the HO parameters only and the HO parameters and random fiber field, respectively. The solid line represents the mean response, whereas the shaded region represents the mean ± standard deviation. One can observe more variations for the volume on the upper limit for the second experiment, as expected since the inclusion of a random fiber field increases uncertainty. The right panel of Figure 4 shows the distributions of the end-diastolic volume obtained for the two cases, where one can observe its asymmetry (for both cases) and the fact that the HO+KL case presents more spread towards larger volume values.

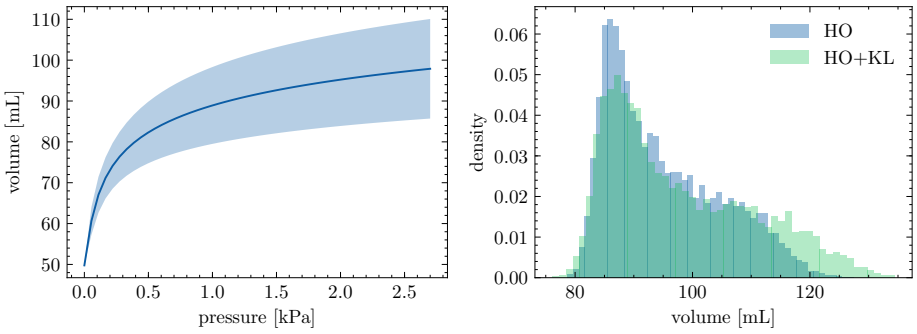

Fig. 4. (Left) Forward uncertainty quantification for the pressure-volume curve during the passive filling stage of the left ventricle dynamics for the parameters of the HO model (only) and HO+KL for the case with random fiber field. The solid line represents the mean value, and the shaded region the confidence interval within one standard deviation. (Right) Distributions of the end-diastolic volume.

Table 2 shows some statistics estimated from the PCE surrogate models for the end-diastolic volume and average fiber strain. In general, local variations in the fiber orientation can significantly impact the outputs. The expected EDV volume value in both cases is very similar, with a slight increase in the coefficient of variation in experiment 2 concerning experiment 1. The average fiber strain ε_{fiber} resulted in a smaller expected value for the second experiment. This reduced fiber strain is a result of the inclusion of uncertainties in the fiber field combined with the fact that it consists of an averaged quantity over a set of elements in the LV.

4.4 Sensitivity Analysis

Finally, we present a global sensitivity analysis based on Sobol indices for experiment 1 dealing with the four parameters of the transversely isotropic HO

ICCS Camera Ready Version 2022
To cite this paper please use the final published version:
DOI: 10.1007/978-3-031-08760-8_61

Table 2. Propagated uncertainties on the quantities of interest (EDV and ε_{fiber}) for experiments 1 (HO) and 2 (HO+KL). The coefficient of variation denotes the ratio between standard deviation and expected value.

Experiment	**Exp. 1**		**Exp. 2**	
Statistics	EDV	ε_{fiber}	EDV	ε_{fiber}
Expected value	94.992	0.138	97.890	0.079
Standard deviation	9.456	0.035	12.188	0.041
Coefficient of Variation	0.099	0.254	0.125	0.518

model. The computation of the main and total Sobol indices was carried out using the PCE surrogate models for EDV and ε.

Table 3. Sensitivity analysis via main and total Sobol indices for the end-diastolic volume and average fiber strain quantities of interest.

Parameters	**End-diastolic volume**		**Average fiber strain**	
	Main	Total	Main	Total
a	0.04109086	0.04786979	0.04350967	0.05388241
b	0.91614816	0.93681466	0.92107288	0.93461802
a_f	0.00537262	0.01050244	0.00269112	0.01456773
b_f	0.01411364	0.02808783	0.01202287	0.01763529

Table 3 presents the main and total Sobol indices for the a, b, a_f, and b_f parameters with respect to end-diastolic volume and average fiber strain. The results show that the b parameter present in Eq. (4) is the one that clearly has the most impact on the QoIs analyzed. It is also worth noting through the total Sobol indices that some level of interaction between the parameters is also present.

5 Conclusions

In this work, we presented a forward uncertainty quantification and sensitivity analysis of a constitutive model usually employed in finite element analysis of cardiac mechanics. In particular, we focused on the passive filling problem of the left ventricle and its derived quantities of interest, such as cavity volume and strain. The analyses explored as uncertain inputs the constitutive parameters of the Holzapfel-Ogden model and the fiber orientation field that defines the cardiac microstructure as a random field using the Karhunen-Loève expansion. Due to the high computational cost of solving the passive filling problem of the LV, the UQ and SA studies were carried out with the surrogate models based on polynomial chaos expansions.

The UQ and SA results can be summarized in the following findings. The model outputs analyzed in this work were highly sensitive to local variations and

ICCS Camera Ready Version 2022
To cite this paper please use the final published version:
DOI: 10.1007/978-3-031-08760-8_61

uncertainties in the fiber orientation. The inclusion of local variations in the fiber field increased the upper limit of the range of uncertainty for the end-diastolic volume. The parameter appearing in the exponent of the isotropic term of the transversely isotropic Holzapfel-Ogden constitutive model is the most sensitive parameter in the material model considered in this work.

5.1 Limitations and Future Works

Some limitations of this work are worthy of discussion for improvements in future works. One of the main limitations of this work is the fact that only the fiber orientation was treated as a random field, in spite of the fact the cardiac tissue is usually modeled as an orthotropic material. This limitation comes from the fact that perturbing the fiber, sheet, and normal directions simultaneously would demand a more complex approach for applying the KL expansion and keeping the orthogonality between the vectors defining these directions. As a consequence of this first limitation, the Holzapfel-Ogden model was limited to the transversely isotropic case. Future works should overcome these limitations by exploring all the parameters in the HO model, including uncertainty in the entire local microstructural vectors of cardiac tissue, including other quantities of interest, and also studying the entire cardiac cycle. Another limitation of this work is the choice of the distributions of the uncertain model parameters. Although it is based on a set of reference values of the literature, further studies should consider an inverse uncertainty quantification approach to better characterize parameter distributions.

References

1. Bayer, J.D., Blake, R.C., Plank, G., Trayanova, N.A.: A novel rule-based algorithm for assigning myocardial fiber orientation to computational heart models. Annals of biomedical engineering **40**(10), 2243–2254 (2012)
2. Cai, L., Ren, L., Wang, Y., Xie, W., Zhu, G., Gao, H.: Surrogate models based on machine learning methods for parameter estimation of left ventricular myocardium. Royal Society open science **8**(1), 201121 (2021)
3. Campos, J., Sundnes, J., Dos Santos, R., Rocha, B.: Uncertainty quantification and sensitivity analysis of left ventricular function during the full cardiac cycle. Philosophical Transactions of the Royal Society A **378**(2173), 20190381 (2020)
4. Campos, J.O., Sundnes, J., Dos Santos, R.W., Rocha, B.M.: Effects of left ventricle wall thickness uncertainties on cardiac mechanics. Biomechanics and modeling in mechanobiology **18**(5), 1415–1427 (2019)
5. Feinberg, J., Langtangen, H.P.: Chaospy: An open source tool for designing methods of uncertainty quantification. Journal of Computational Science **11**, 46–57 (2015)
6. Guccione, J.M., Costa, K.D., McCulloch, A.D.: Finite element stress analysis of left ventricular mechanics in the beating dog heart. Journal of biomechanics **28**(10), 1167–1177 (1995)

ICCS Camera Ready Version 2022
To cite this paper please use the final published version:
DOI: 10.1007/978-3-031-08760-8_61

7. Holzapfel, G.A., Ogden, R.W.: Constitutive modelling of passive myocardium: a structurally based framework for material characterization. Philosophical Transactions of the Royal Society A: Mathematical, Physical and Engineering Sciences **367**(1902), 3445–3475 (2009)
8. Karlsen, K.S.: Effects of inertia in modeling of left ventricular mechanics. Master's thesis (2017)
9. Kovacheva, E., Gerach, T., Schuler, S., Ochs, M., Dössel, O., Loewe, A.: Causes of altered ventricular mechanics in hypertrophic cardiomyopathy—an in-silico study (2021)
10. Levrero-Florencio, F., Margara, F., Zacur, E., Bueno-Orovio, A., Wang, Z., Santiago, A., Aguado-Sierra, J., Houzeaux, G., Grau, V., Kay, D., et al.: Sensitivity analysis of a strongly-coupled human-based electromechanical cardiac model: Effect of mechanical parameters on physiologically relevant biomarkers. Computer methods in applied mechanics and engineering **361**, 112762 (2020)
11. Logg, A., Mardal, K.A., Wells, G.: Automated solution of differential equations by the finite element method: The FEniCS book, vol. 84. Springer Science & Business Media (2012)
12. Mosqueira, D., Smith, J.G., Bhagwan, J.R., Denning, C.: Modeling hypertrophic cardiomyopathy: mechanistic insights and pharmacological intervention. Trends in molecular medicine **25**(9), 775–790 (2019)
13. Oliveira, R.S., Alonso, S., Campos, F.O., Rocha, B.M., Fernandes, J.F., Kuehne, T., dos Santos, R.W.: Ectopic beats arise from micro-reentries near infarct regions in simulations of a patient-specific heart model. Scientific reports **8**(1), 1–14 (2018)
14. Osnes, H., Sundnes, J.: Uncertainty analysis of ventricular mechanics using the probabilistic collocation method. IEEE transactions on biomedical engineering **59**(8), 2171–2179 (2012)
15. Rodríguez-Cantano, R., Sundnes, J., Rognes, M.E.: Uncertainty in cardiac myofiber orientation and stiffnesses dominate the variability of left ventricle deformation response. International journal for numerical methods in biomedical engineering **35**(5), e3178 (2019)
16. Saltelli, A., Ratto, M., Andres, T., Campolongo, F., Cariboni, J., Gatelli, D., Saisana, M., Tarantola, S.: Global sensitivity analysis: the primer. John Wiley & Sons (2008)

ICCS Camera Ready Version 2022
To cite this paper please use the final published version:
DOI: 10.1007/978-3-031-08760-8_61